Supporting Information

Light-induced Charge Separation in Densely Packed Donor-Acceptor Coordination Cages

Marina Frank, Jennifer Ahrens, Isabel Bejenke, Marcel Krick, Dirk Schwarzer, Guido H. Clever*

Contents

A) Synthesis

Synthesis of ligand A', double cage $[3BF_4@Pd_4A'_8]^{5+}$, mixture of homo-octameric double cages $[3BF_4@Pd_4D_8]^{5+}$ + $[3BF_4@Pd_4A'_8]^{5+}$ and the mixed-ligand double cages $[3BF_4@Pd_4D_mA'_{8-m}]^{5+}$

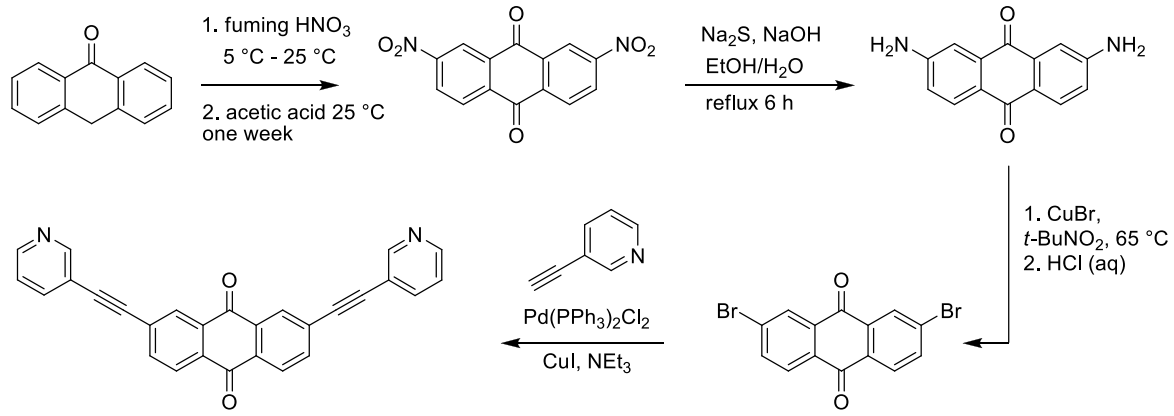

Figure SI-1: Synthetic route to ligand **A'**. For the synthesis procedure of the first three steps see the literature. [1],[2]

A suspension of 2,7-dibromo-9,10-anthraqinone (140 mg, 0.38 mmol, 1.00 eq.), 3-ethinylpyridine (118 mg, 1.15 mmol, 3.0 eq.), copper(I)iodide (7 mg, 0.04 mmol, 0.10 eq.) in NEt_3 (15 mL) was degassed using the "pump and freeze" method. $Pd(PPh_3)_2Cl_2$ (27 mg, 0.04 mmol, 0.10 eq.) was added and the reaction mixture was stirred for 18 h at 90 °C. After heating, the solvent was removed and the crude product was prepurified by column chromatography ($CHCl_3$:MeOH 50:1). After recrystallization from pyridine the product was isolated as a pale yellow solid (92 mg, 0.22 mmol, 59 %).

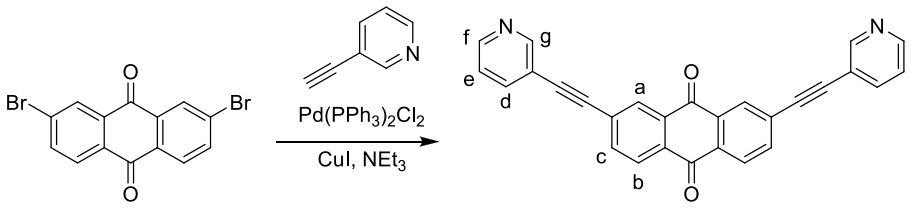

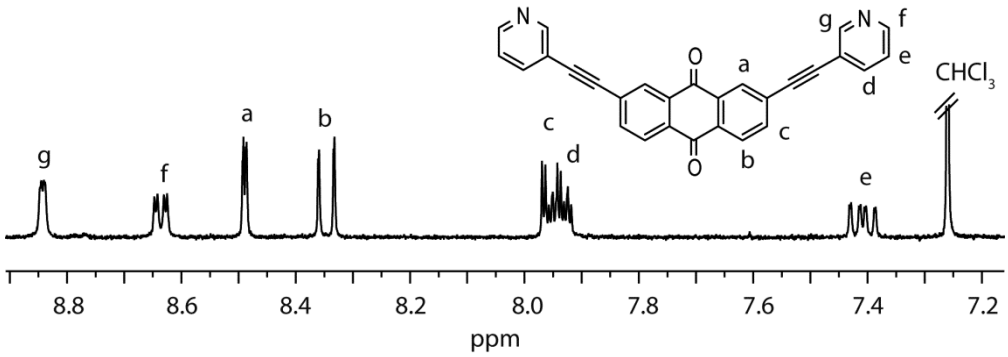

Figure SI-2: ^{1}H NMR (300 MHz, 298 K, chloroform-*d*) of ligand **A**'.

^{1}H NMR (300 MHz, chloroform-*d*) δ [ppm] = 8.83 (d, J = 1.9 Hz, 2H, H_g), 8.63 (dd, J = 5.0, 1.7 Hz, 2H, H_f), 8.48 (d, J = 1.7 Hz, 2H, H_a), 8.34 (d, J = 8.1 Hz, 2H, H_b), 7.94 (dd, J = 8.1, 1.8 Hz, 2H, H_c), 7.88 (dt, J = 8.0, 1.8 Hz, 2H, H_d), 7.36 (dd, J = 7.9, 5.0 Hz, 2H, H_e).

ESI-MS [*m/z*]: found 411.1 (100 %), 412.1 (31 %), 413.1 (6 %); calculated for $[C_{28}H_{15}N_2O_2]^+$ 411.1 (100 %), 412.1 (31 %), 413.1 (5 %).

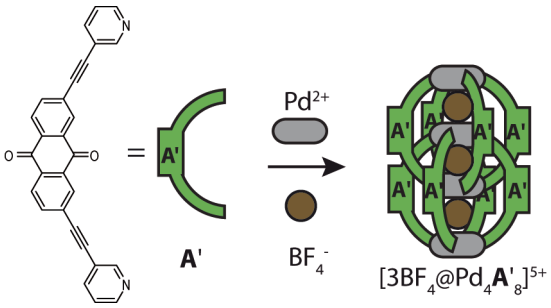

Ligand **A**' (1.15 mg. 2.8 µmol) was suspended in 1 mL CD_3CN and 95 µL of 15 mM $[Pd(CH_3CN)_4](BF_4)_2$ stock solution in CD_3CN were added to the suspension. The reaction mixture was stirred at 70 °C for 18 h to obtain the double cage $[3BF_4@Pd_4\mathbf{A'}_8]^{5+}$ in quantitative yield. The borderline solubility of the cage caused some precipitation when the sample was cooled to room temperature. This problem was resolved by introducing solubilizing groups into the ligand (see below).

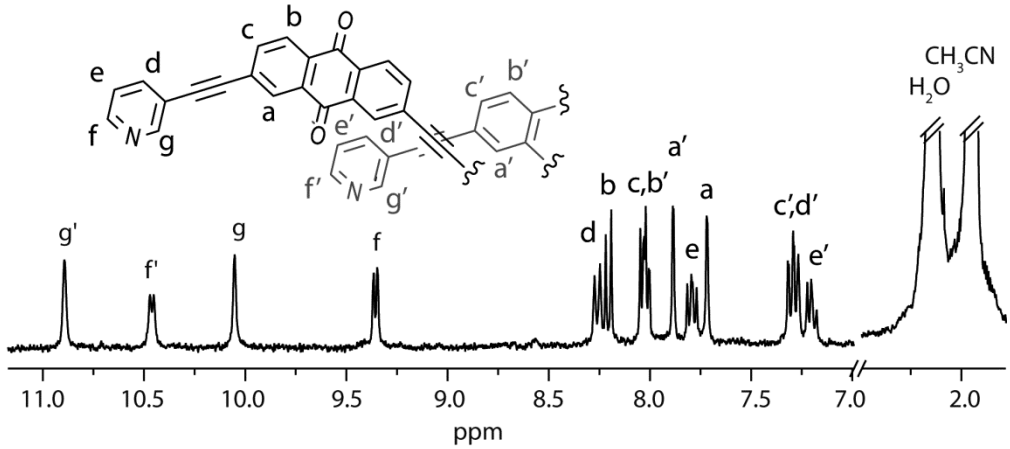

Figure SI-3: ^{1}H NMR (300 MHz, 298 K, acetonitrile-d_3) of the double cage $[3BF_4@Pd_4\mathbf{A'}_8]^{5+}$.

^{1}H NMR (500 MHz, 298 K, acetonitrile-d_3) δ [ppm] = 10.88 (s, 8H, $H_{g'}$), 10.45 (d, J = 6.0 Hz, 8H, $H_{f'}$), 10.04 (s, 8H, H_g), 9.32 (d, J = 6.3 Hz, 8H, H_f), 8.25 (d, J = 8.1 Hz, 8H, H_d), 8.20 (d, J = 7.8 Hz, 8H, H_b), 8.06 – 7.98 (m, 16H, H_c, $H_{b'}$), 7.87 (s, 8H, $H_{a'}$), 7.82 – 7.75 (m, 8H, H_e), 7.71 (s, 8H, H_a), 7.33 – 7.24 (m, 16H, $H_{c'}$, $H_{d'}$), 7.23 – 7.15 (m, 8H, $H_{e'}$).

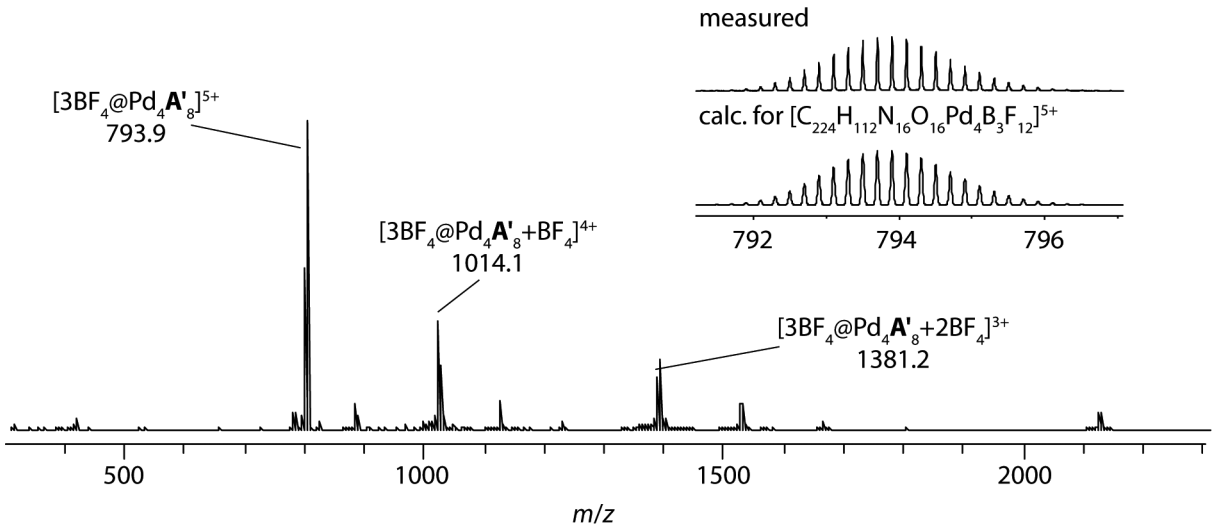

Figure SI-4: ESI high resolution mass spectrum of the double cage $[3BF_4@Pd_4\mathbf{A'}_8]^{5+}$.

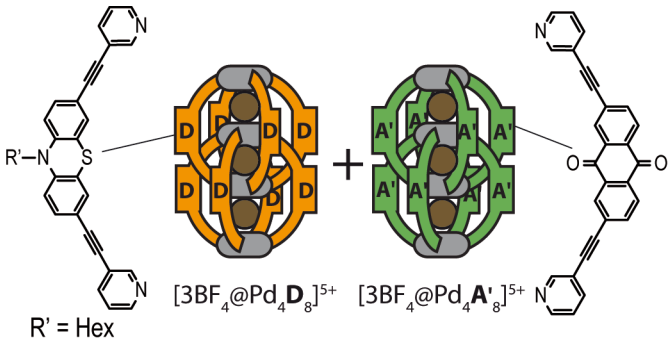

The mixture of homo-octameric double cages was prepared by mixing 250 µL of 0.35 mM double cage $[3BF_4@Pd_4\mathbf{D}_8]^{5+}$ solution in CD_3CN with 250 µL of 0.35 mM double cage $[3BF_4@Pd_4\mathbf{A'}_8]^{5+}$ solution in CD_3CN.

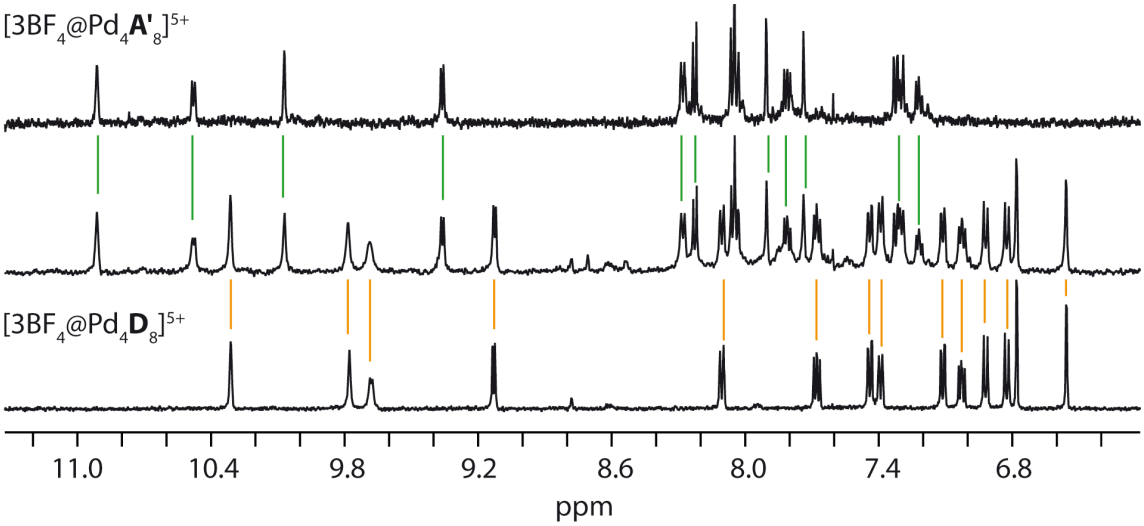

Figure SI-5: ^{1}H NMR (500 MHz, 298 K, acetonitrile-d_3) of the double cage mixture $[3BF_4@Pd_4\mathbf{D}_8]^{5+}$ and $[3BF_4@Pd_4\mathbf{A}'_8]^{5+}$.

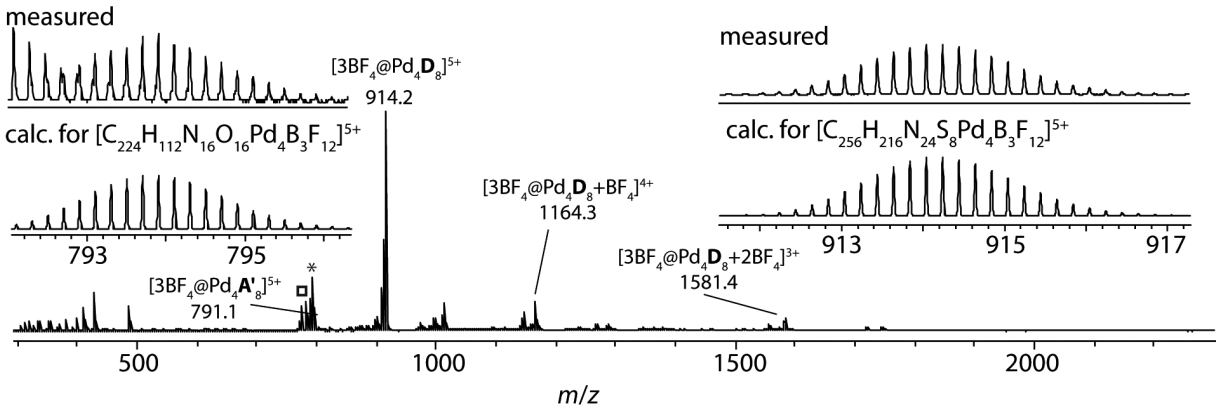

Figure SI-6: ESI high resolution mass spectra of the double cage mixture $[3BF_4@Pd_4\mathbf{D}_8]^{5+}$ and $[3BF_4@Pd_4\mathbf{A}'_8]^{5+}$. * denotes bromide contaminated species $[2Br+BF_4@Pd_4\mathbf{A}'_8]^{5+}$; □ denotes chloride contaminated species $[2Cl+BF_4@Pd_4\mathbf{A}'_8]^{5+}$.

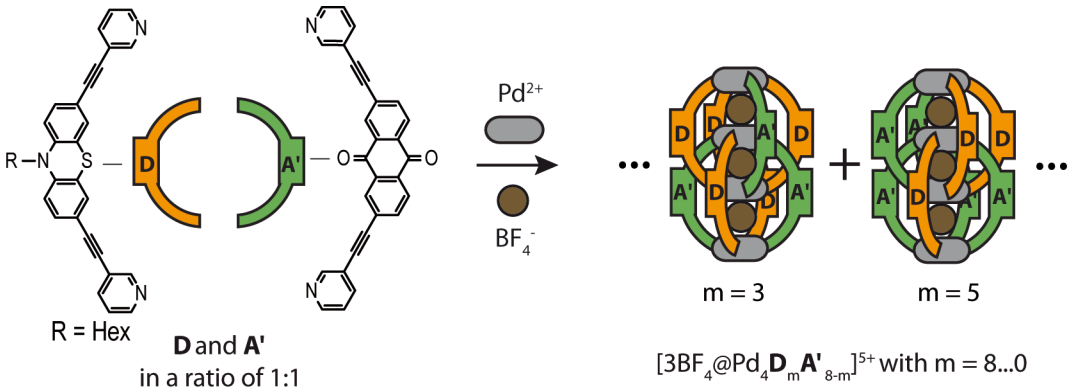

The mixed-ligand double cages were prepared by mixing ligand **D** (1.36 mg) and ligand **A'** (1.15 mg) in 2 mL of deuterated acetonitrile with 190 µL of 15 mM $[Pd(CH_3CN)_4](BF_4)_2$ stock solution and heating the mixture at 70 °C for 18 h.

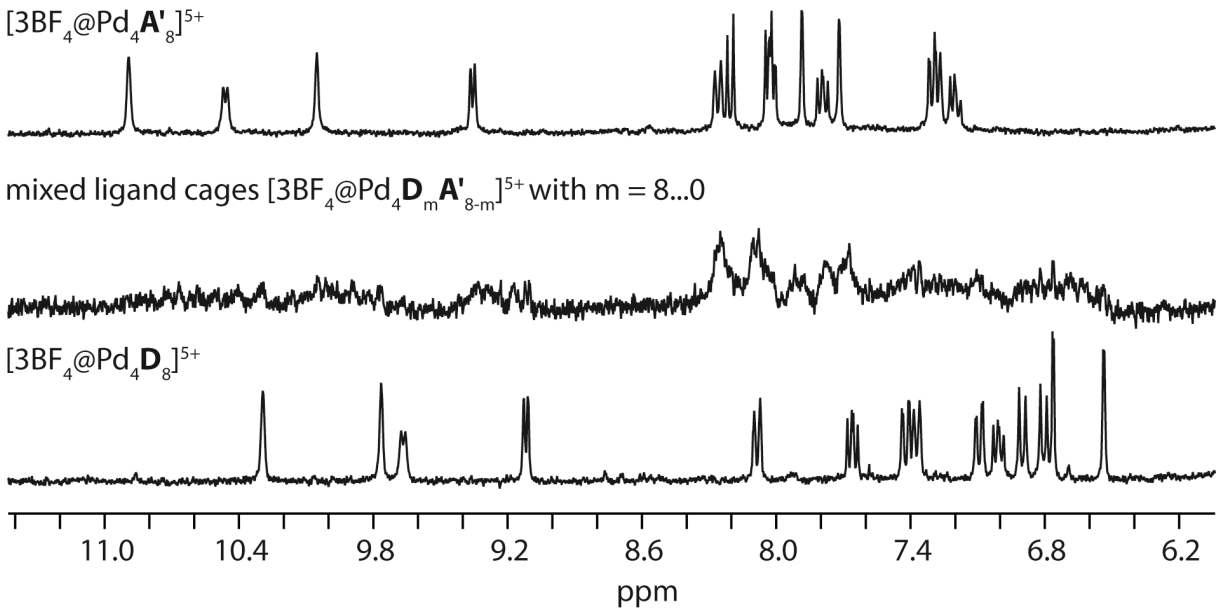

Figure SI-7: ^{1}H NMR (300 MHz, 298 K, acetonitrile-d_3) of the mixed-ligand double cage $[3BF_4@Pd_4\mathbf{D}_m\mathbf{A'}_{8-m}]^{5+}$ with m = 8…0.

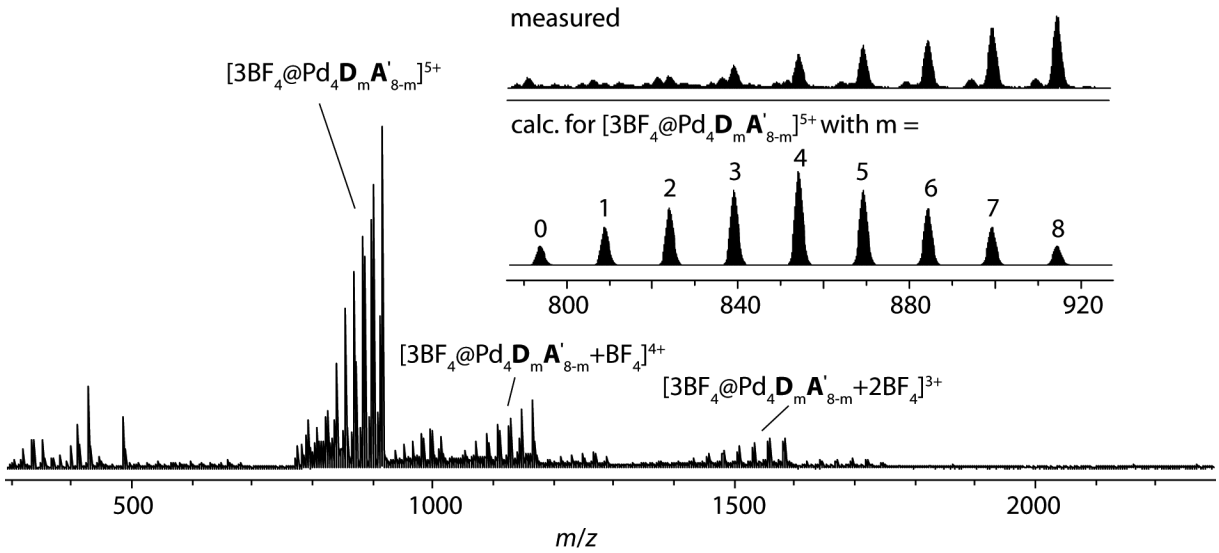

Figure SI-8: ESI high resolution mass spectra of the mixed-ligand cages $[3BF_4@Pd_4\mathbf{D}_m\mathbf{A'}_{8-m}]^{5+}$ with m = 8…0. The different solubility of the ligands proved to complicate the formation of a statistically distributed cage mixture. Therefore, solubilizing groups were attached to the anthraquinone ligand as described in the following paragraph.

Synthesis of ligand A, double cage $[3BF_4@Pd_4A_8]^{5+}$, mixture of homo-octameric double cages $[3BF_4@Pd_4D_8]^{5+}$ + $[3BF_4@Pd_4A_8]^{5+}$ and the mixed-ligand double cages $[3BF_4@Pd_4D_mA_{8-m}]^{5+}$

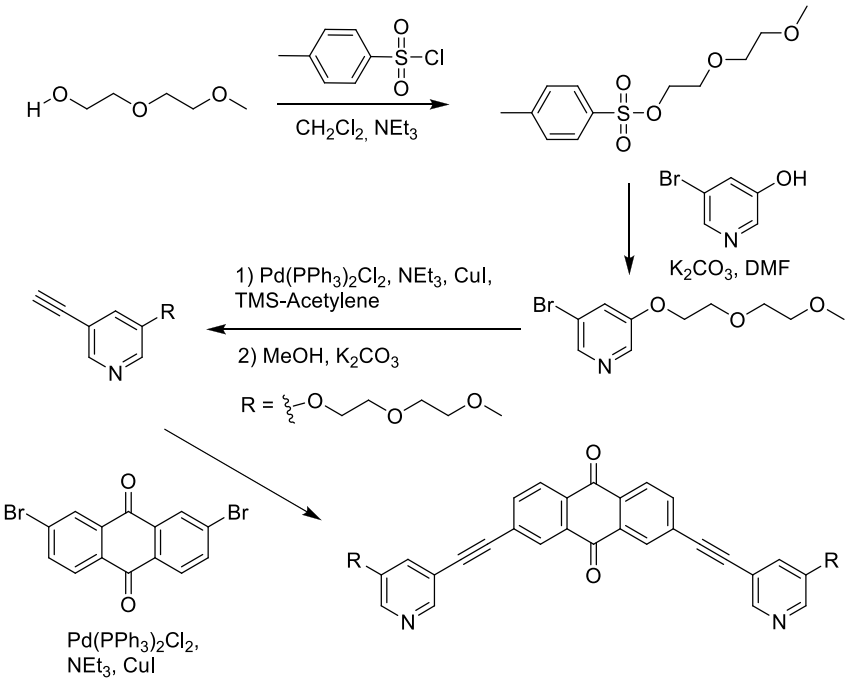

Figure SI-9: Synthetic route to the modified anthraquinone ligand **A**.

2-(2-Methoxyethoxy)ethanol (15.0 g, 125 mmol, 1.00 eq.) was dissolved with tosylchloride (23.8 g, 125 mmol, 1.00 eq.) in triethylamine (60 mL) and CH_2CL_2 (100 mL). After 12 h of stirring a white precipitate was filtrated off and the residue was washed with ethyl acetate. The solvent was removed from the filtrate and the crude product was purified by column chromatography (hexane : ethylacetate = 1 : 1). The clean product was obtained as a yellowish oil (26.8 g, 98 mmol, 78 %).

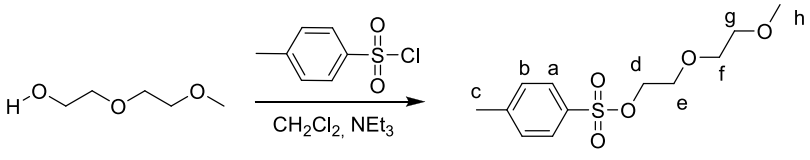

^{1}H NMR (300 MHz, 298 K, chloroform-*d*) δ [ppm] = 7.79 – 7.72 (m, 2H, H_b), 7.33 – 7.27 (m, 2H, H_a), 4.15 – 4.10 (m, 2H, H_d), 3.67 – 3.62 (m, 2H, H_e), 3.55 – 3.40 (m, 4H, H_f, H_g), 3.30 (s, 3H, H_h), 2.40 (s, 3H, H_c).

ESI-MS [*m/z*]: found 275.1; calculated for $[C_{12}H_{18}SO_5+H]^+$ 275.1.

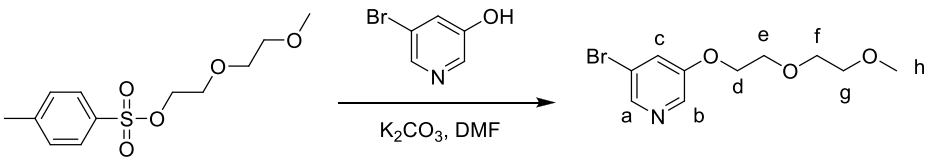

5-Bromo-3-pyridinole (1.00 g, 5.75 mmol, 1.00 eq.), 2-(2-methoxyethoxy)ethyl-4-methylbenzenesulfonate (2.36 g, 8.62 mmol, 1.50 eq.), K_2CO_3 (2.38 g, 17.24 mmol, 3.00 eq.) and DMF (20 mL) were mixed and heated to 70 °C for 18 h. After the reaction has completed, the mixture was poured into 2 M NaOH and the product was extracted with EtOAc. The crude product was purified by column chromatography with chloroform : methanol = 10 : 1 and was isolated as a brownish oil (2.20 g, 7.97 mmol, 92 %).

^{1}H NMR (300 MHz, 298 K, chloroform-*d*) δ [ppm] = 8.33 – 8.26 (m, 2H), 7.52 (s, 1H), 4.24 – 4.17 (m, 2H), 3.90 – 3.82 (m, 2H), 3.74 – 3.65 (m, 2H), 3.59 – 3.52 (m, 2H), 3.38 (s, 3H).

ESI-MS [*m/z*]: found 276.0 (100), 277.0 (11), 278.0 (100), 279.0 (11); calculated for $[C_{10}H_{12}NO_3Br+H]^+$ 276.0 (100), 277.0 (11), 278.0 (100), 279.0 (11).

3-Bromo-5-(2-(2-methoxyethoxy)ethoxy)pyridine (2.20 g, 7.97 mmol, 1.00 eq.) was dissolved in 10 mL of NEt_3 and CuI (151 mg, 0.80 mmol, 0.10 eq.) was added. After the mixture was degassed by using the „freeze and pump“-method, $Pd(PPh_3)_2Cl_2$ (559 mg, 0.80 mmol, 0.10 eq.) and trimethylsilylacetylene (3.30 mL, 23.91 mmol, 3.00 eq.) were added. The reaction mixture was heated to 90 °C for 18 h. The solvent was removed and the crude product was purified by column chromatography. The TMS-protecting group was removed by stirring the product with K_2CO_3 (3 g, 21.43 mmol, 2.69 eq.) in methanol (10 mL).

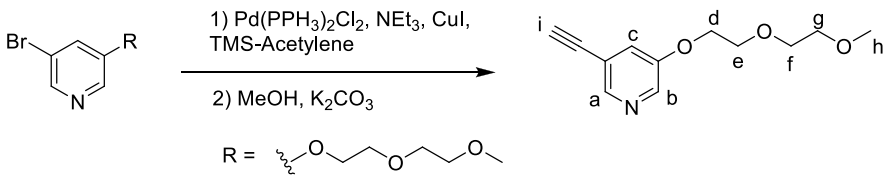

^{1}H NMR (300 MHz, 298 K, chloroform-*d*) δ [ppm] = 8.32 (d, *J* = 1.6 Hz, 1H, H_a), 8.29 (d, *J* = 2.8 Hz, 1H, H_b), 7.30 (dd, *J* = 2.9, 1.6 Hz, 1H, H_c), 4.21 – 4.15 (m, 2H, H_d), 3.90 – 3.84 (m, 2H, H_e), 3.74 – 3.68 (m, 2H, H_f), 3.60 – 3.54 (m, 2H, H_g), 3.39 (s, 3H, H_h), 3.19 (s, 1H, H_i).

ESI-MS [*m/z*]: found 222.1 (100), 223.1 (14); calculated for $[C_{12}H_{15}NO_3+H]^+$ 222.1 (100), 223.1 (14).

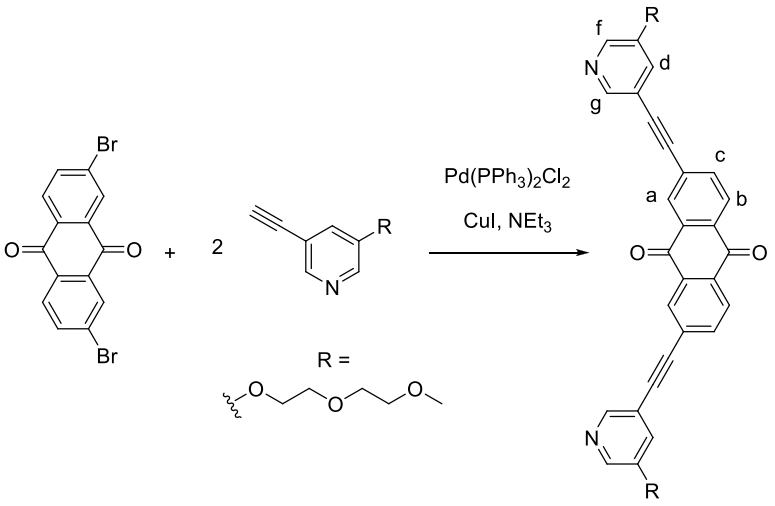

2,7-Dibromoanthraquinone (100 mg, 0.27 mmol, 1.00 eq.) was mixed with 3-ethynyl-5-(2-(2-methoxyethoxy)ethoxy) pyridine (121 mg, 0.55 mmol, 2.00 eq.), copper(I)iodid (10 mg, 0.05 mmol, 0.19 eq.) in 10 mL triethylamine. The mixture was degassed by using the „freeze and pump"-method and $Pd(PPh_3)_2Cl_2$ (19 mg, 0.03 mmol, 0.10 eq.) was added. The reaction mixture was heated to 90 °C for 18 h. The solvent was removed and the crude product was purified by column chromatography (EtOAc -> 10 % MeOH in EtOAc). The product was isolated as yellow solid (110 mg, 0.17 mmol, 62 %).

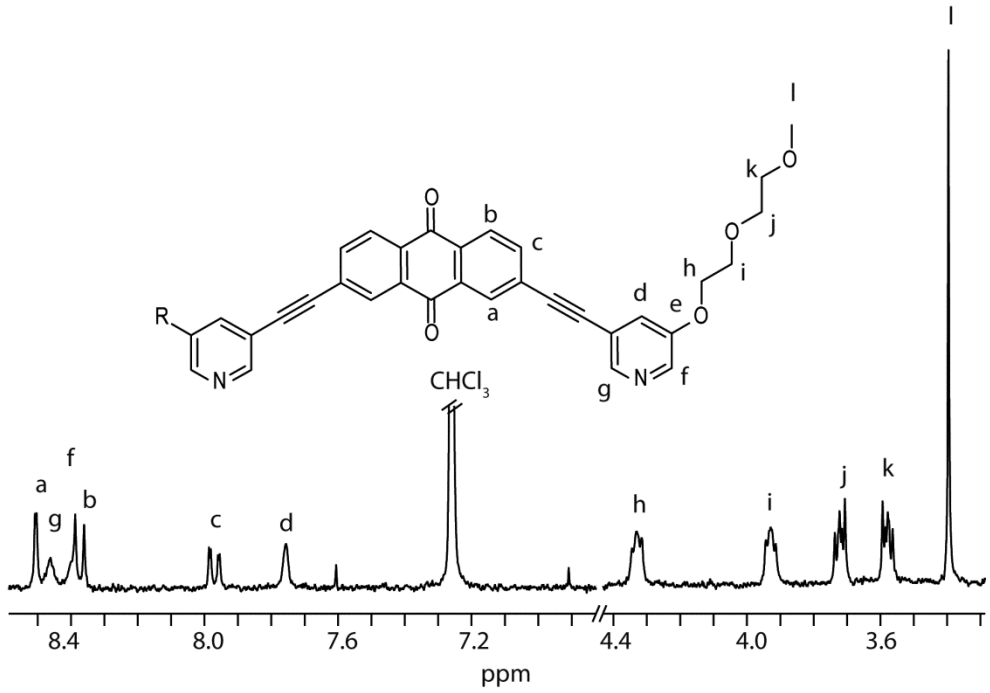

Figure SI-10: ^{1}H NMR (300 MHz, 298 K, chloroform-*d*) of ligand **A**.

^{1}H NMR (300 MHz, 298 K, chloroform-*d*) δ [ppm] = 8.50 (s, 2H, H_a), 8.46 (s, 2H, H_g), 8.40 (s, 2H, H_f), 8.37 (d, J = 8.1 Hz, 2H, H_b), 7.97 (d, J = 8.8 Hz, 2H, H_c), 7.76 (s, 2H, H_d), 4.37 – 4.28 (m, 4H, H_h), 3.96 – 3.89 (m, 4H, H_i), 3.75 – 3.68 (m, 4H, H_j), 3.61 – 3.55 (m, 4H, H_k), 3.40 (s, 6H, H_l).

ESI-MS [*m/z*]: found 647.2 (100 %), 648.2 (41 %), 649.2 (8 %); calculated for $[C_{38}H_{34}N_2O_8]^+$ 647.2 (100 %), 648.2 (42 %), 649.2 (10 %).

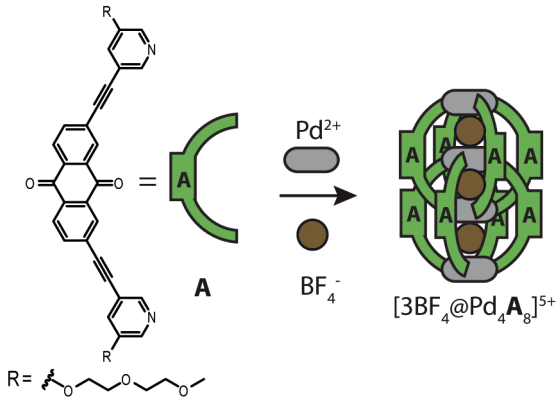

Ligand **A** (1.81 mg, 2.8 µmol) was suspended in 1 mL CD_3CN and 95 µL of 15 mM $[Pd(CH_3CN)_4](BF_4)_2$ stock solution were added to the suspension. The reaction mixture was stirred at 70 °C for 18 h to obtain the double cage $[3BF_4@Pd_4\mathbf{A}_8]^{5+}$ in quantitative yield.

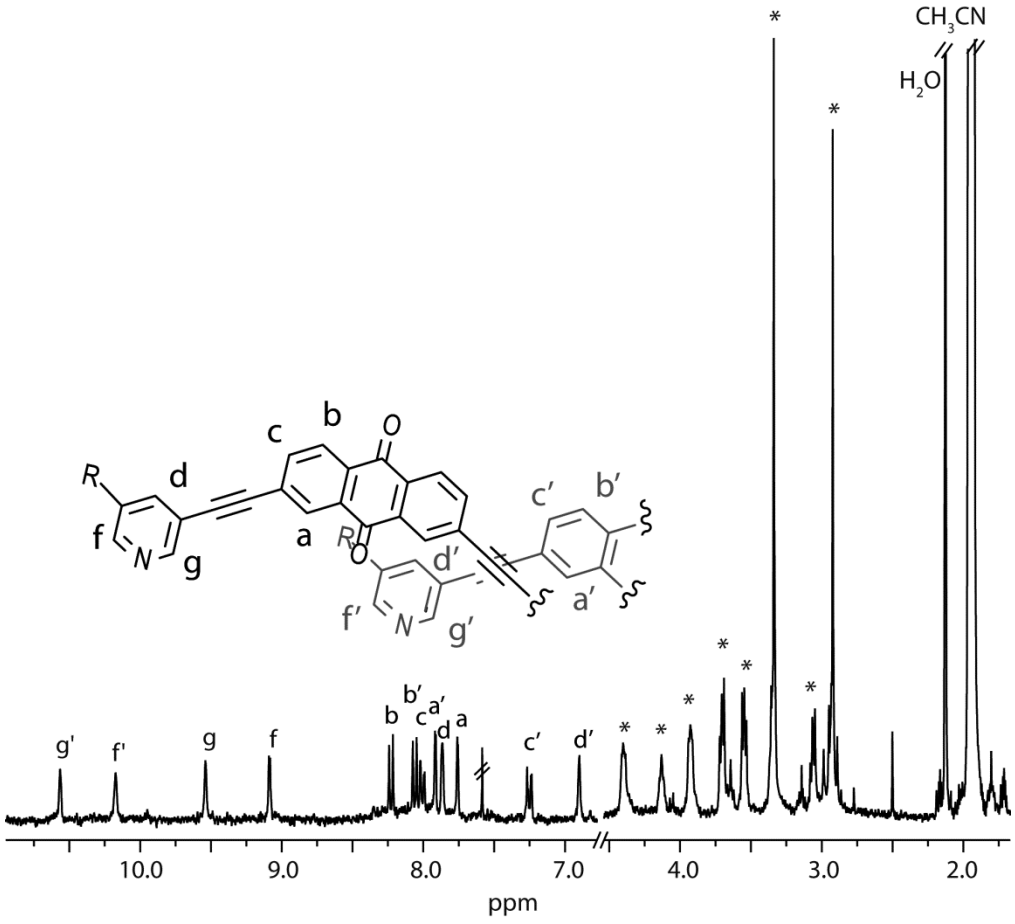

Figure SI-11: ^{1}H NMR (300 MHz, 298 K, acetonitrile-d_3) of the double-cage $[3BF_4@Pd_4\mathbf{A}_8]^{5+}$. * denotes the signals of the PEG chains.

^{1}H NMR (300 MHz, 298 K, acetonitrile-d_3) δ [ppm] = 10.56 (s, 8H, $H_{g'}$), 10.17 (s, 8H, $H_{f'}$), 9.54 (s, 8H, H_g), 9.09 (d, J = 2.3 Hz, 8H, H_f), 8.23 (d, J = 8.0 Hz, 8H, H_b), 8.06 (d, J = 7.9 Hz, 8H, $H_{b'}$), 8.01 (dd, J = 8.0, 1.5 Hz, 8H, H_c), 7.91 (d, J = 1.3 Hz, 8H, H_a), 7.87 (d, J = 2.5 Hz, 8H, H_d), 7.76 (s, J = 1.4 Hz, 8H, H_a) 7.25 (dd, J = 8.6, 1.7 Hz, 8H, $H_{c'}$), 6.90 (s, 8H, $H_{d'}$), 4.40 (s, 16H), 4.13 (s, 16H), 3.93 (s, 16H), 3.77 – 3.59 (m, 32H), 3.58 – 3.52 (m, 8H, 16 H), 3.38 – 3.29 (m, 40H), 3.10 – 3.02 (m, 16H), 2.92 (s, 24H).

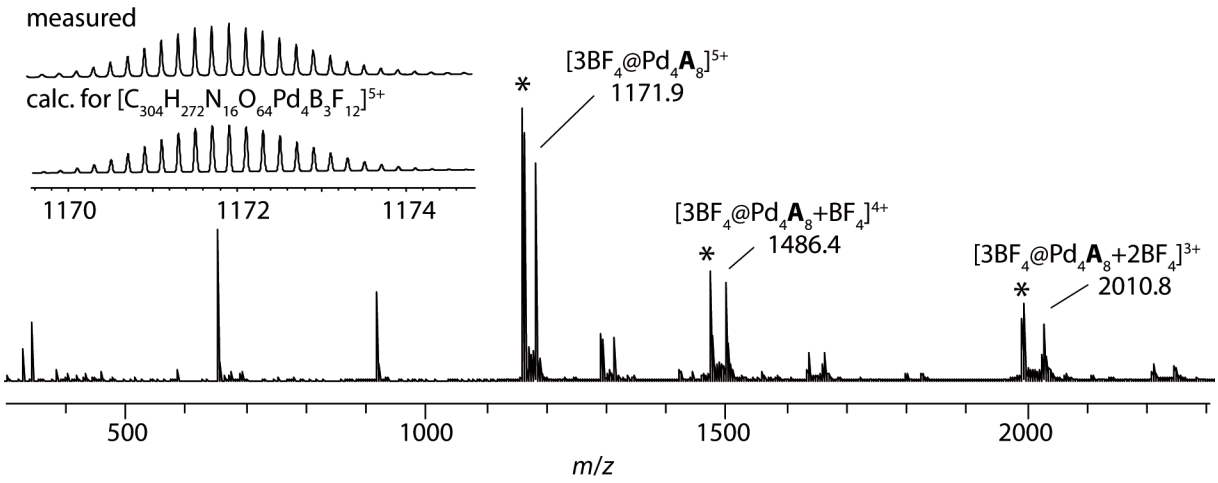

Figure SI-12: ESI high resolution mass spectra of the double cage $[3BF_4@Pd_4\mathbf{A}_8]^{5+}$. * denotes the chloride containing species $[2Cl+BF_4@Pd_4\mathbf{A}_8]^{5+}$.

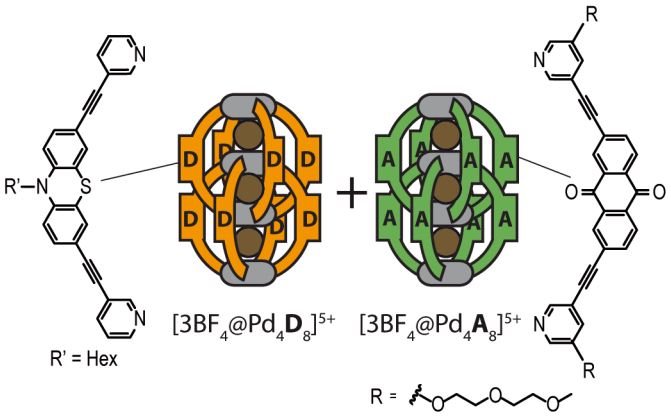

The mixture of homo-octameric double cages was prepared by mixing 250 µL of 0.35 mM double cage $[3BF_4@Pd_4\mathbf{D}_8]^{5+}$ solution in CD_3CN with 250 µL of 0.35 mM double cage $[3BF_4@Pd_4\mathbf{A}_8]^{5+}$ solution in CD_3CN.

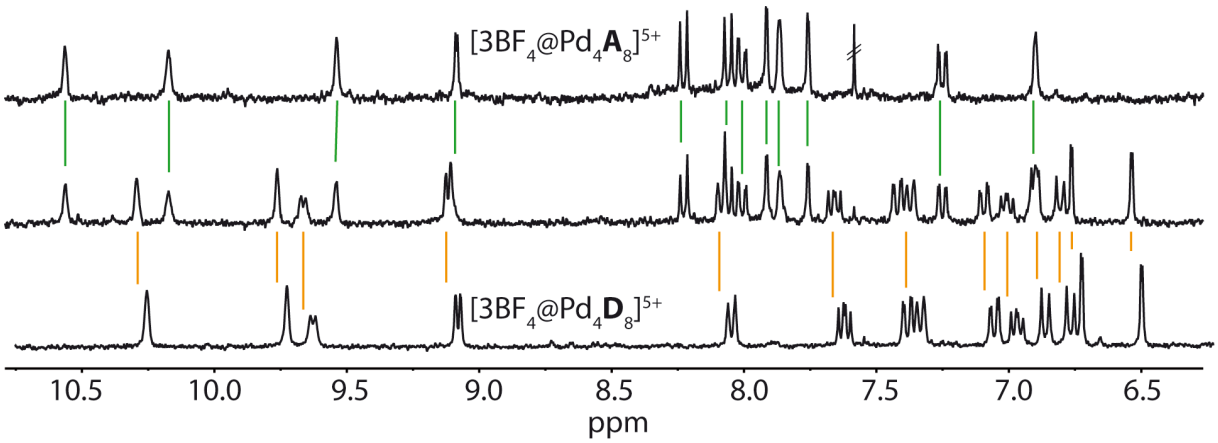

Figure SI-13: ^{1}H NMR (300 MHz, 298 K, acetonitrile-d_3) of the double cage mixture $[3BF_4@Pd_4\mathbf{D}_8]^{5+}$ and $[3BF_4@Pd_4\mathbf{A}_8]^{5+}$.

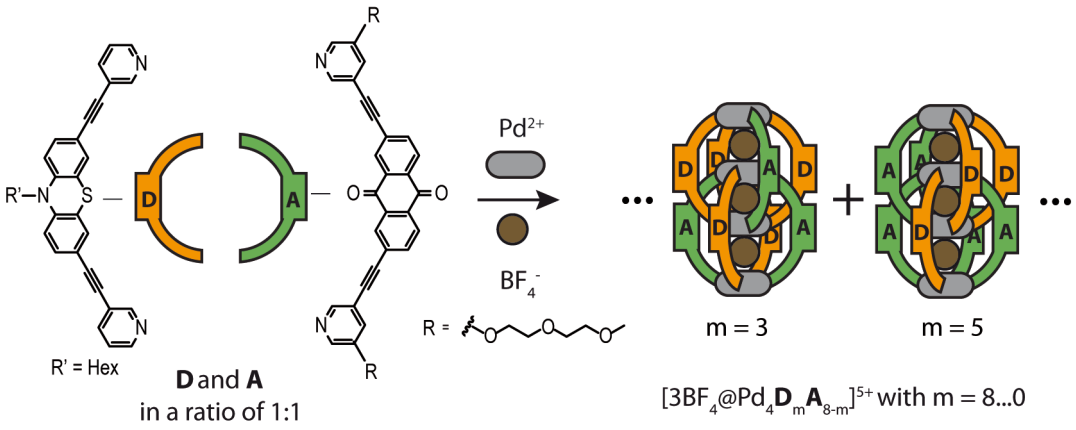

The mixed-ligand double cages were prepared by mixing ligand **D** (1.36 mg) and ligand **A** (1.81 mg) in 2 mL of CD_3CN with 190 µL of 15 mM $[Pd(CH_3CN)_4](BF_4)_2$ stock solution and heating the mixture at 70 °C for 18 h.

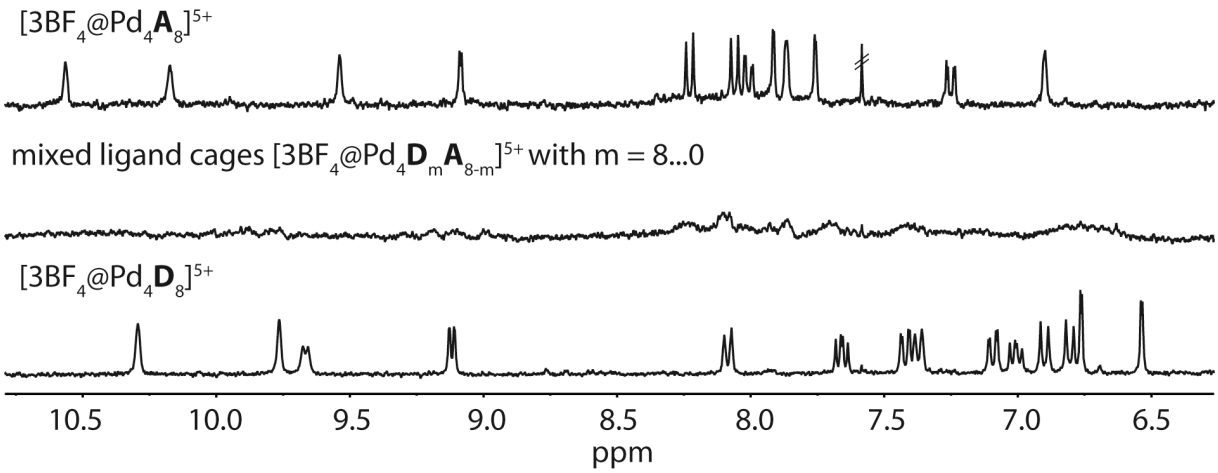

Figure SI-14: ^{1}H NMR (300 MHz, 298 K, acetonitrile-d_3) of mixed-ligand double cage $[3BF_4@Pd_4\mathbf{D}_m\mathbf{A}_{8-m}]^{5+}$ with m = 8...0.

Figure 2b in the main manuscript shows the ESI MS spectrum of the mixed-ligand double cage $[3BF_4@Pd_4\mathbf{D}_m\mathbf{A}_{8-m}]^{5+}$. Owing to the good solubility of ligand **A**, the intended statistical distribution of species was achieved.

B) Geometry optimization of double cage structure $[3BF_4@Pd_4A'_8]^{5+}$

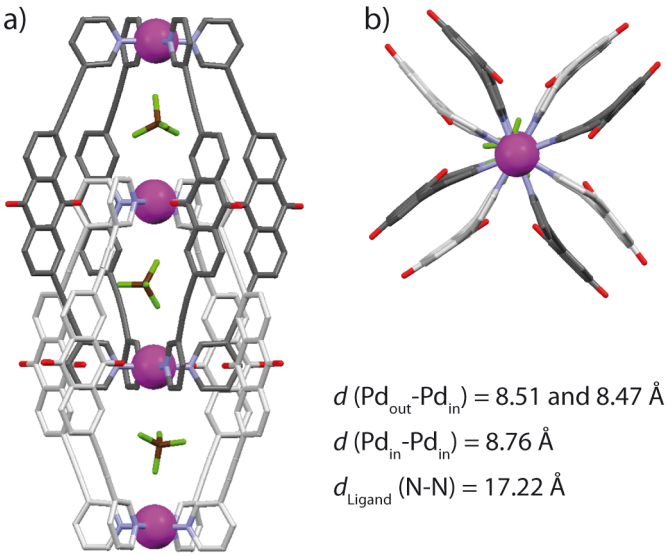

Figure SI-15: DFT calculated model for $[3BF_4@Pd_4\mathbf{A'}_8]^{5+}$ shown in a) side view and b) view along the Pd-Pd axis.

The structure of the double cage $[3BF_4@Pd_4\mathbf{L}^2_8]^{5+}$ was constructed according to the previously reported X-ray structure of the closely related acridone-based double cage.[3] The obtained structure was optimized on ωB97XD/def2-SVP DFT level (charge: +5, multiplicity: singlet, with three BF_4^- inside the three internal pockets, no constraints) using the dispersion-corrected ωB97XD functional implemented in Gaussian '09[4] and the Ahlrich def2-SVP basis set obtained from the EMSL basis set exchange website https://bse.pnl.gov/bse/portal.[5] Hydrogen atoms are omitted for clarity.

C) UV/VIS spectroscopy

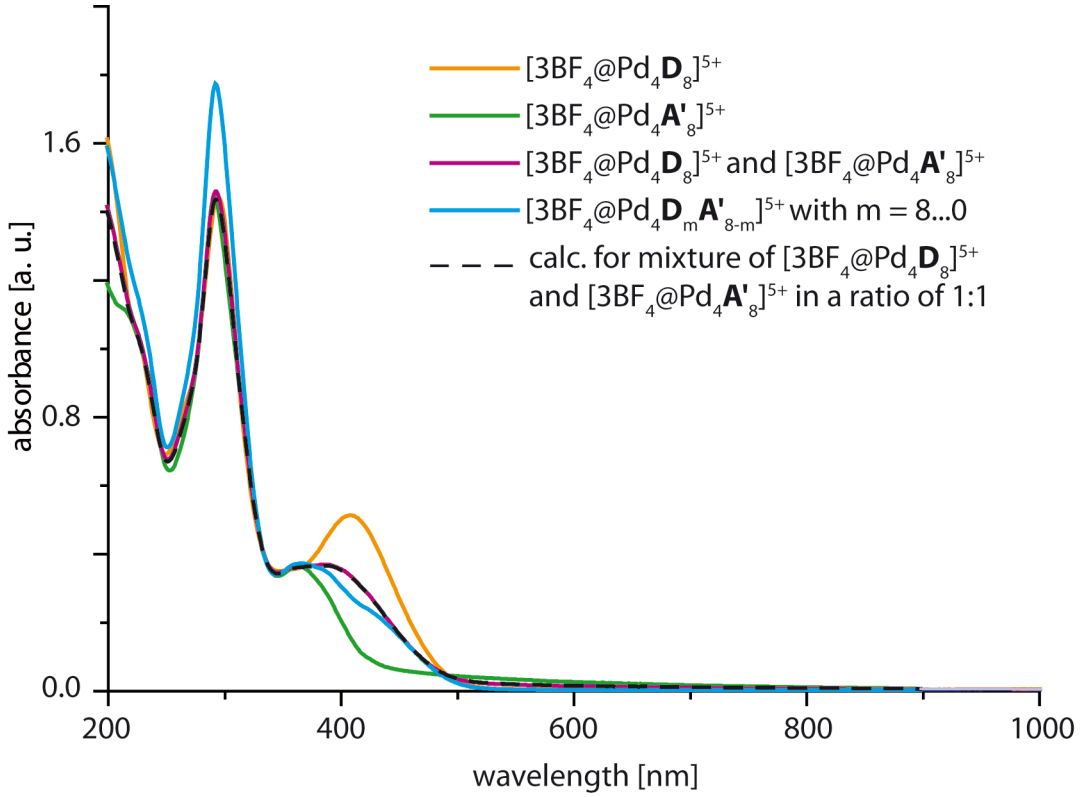

Figure SI-16: UV/Vis spectra of double cages $[3BF_4@Pd_4\mathbf{D}_8]^{5+}$ (20 µM in MeCN) and $[3BF_4@Pd_4\mathbf{A'}_8]^{5+}$ (20 µM in MeCN), their mixture $[3BF_4@Pd_4\mathbf{D}_8]^{5+}$ + $[3BF_4@Pd_4\mathbf{A'}_8]^{5+}$ (10 µM of each double cage in MeCN) and the mixed-ligand cages $[3BF_4@Pd_4\mathbf{D}_m\mathbf{A'}_{8-m}]^{5+}$ (20 µM in MeCN). The spectrum for the mixture of $[3BF_4@Pd_4\mathbf{D}_8]^{5+}$ and $[3BF_4@Pd_4\mathbf{A'}_8]^{5+}$ in a ratio of 1:1 was calculated from experimental spectra of each cage. Cuvette path length: 0.2 cm.

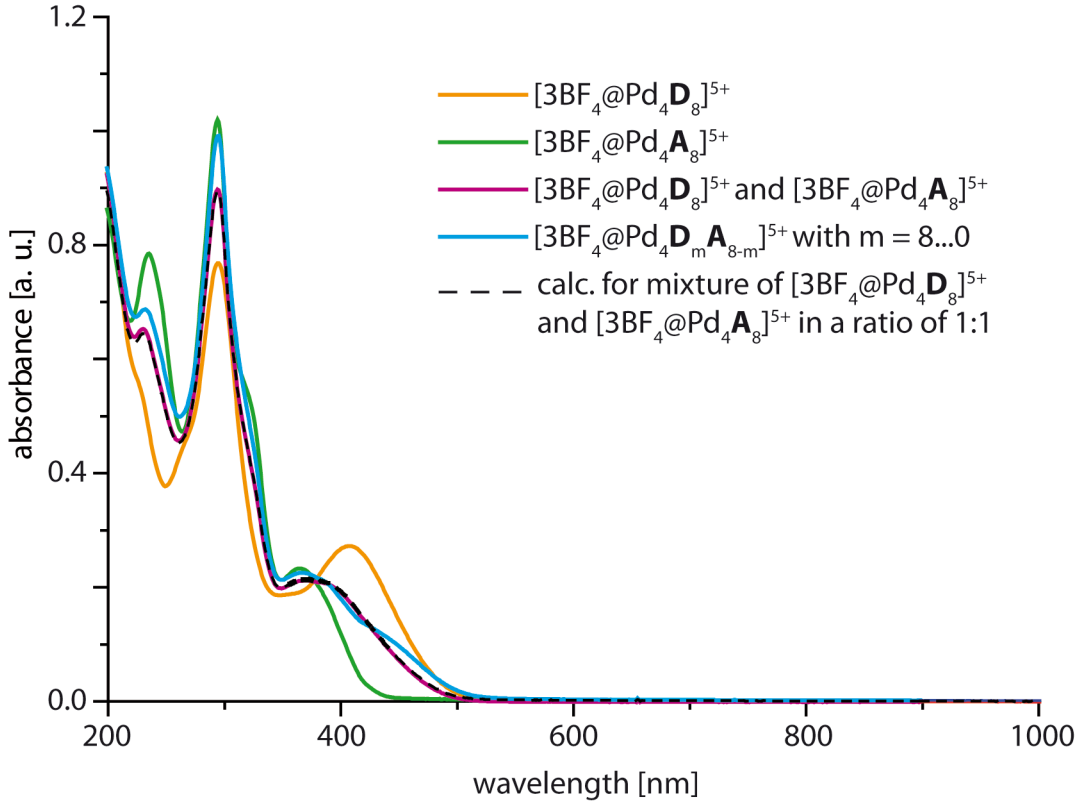

Figure SI-17: UV/Vis spectra of double cages $[3BF_4@Pd_4\mathbf{D}_8]^{5+}$ (20 µM in MeCN) and $[3BF_4@Pd_4\mathbf{A}_8]^{5+}$ (20 µM in MeCN), their mixture $[3BF_4@Pd_4\mathbf{D}_8]^{5+}$ + $[3BF_4@Pd_4\mathbf{A}_8]^{5+}$ (10 µM of each double cage in MeCN) and the mixed-ligand cages $[3BF_4@Pd_4\mathbf{D}_m\mathbf{A}_{8-m}]^{5+}$ (20 µM in MeCN). The spectrum for the mixture of homo-octameric double cages $[3BF_4@Pd_4\mathbf{D}_8]^{5+}$ and $[3BF_4@Pd_4\mathbf{A}_8]^{5+}$ in a ratio of 1:1 was calculated from experimental spectra of each cage. Cuvette path length: 0.1 cm.

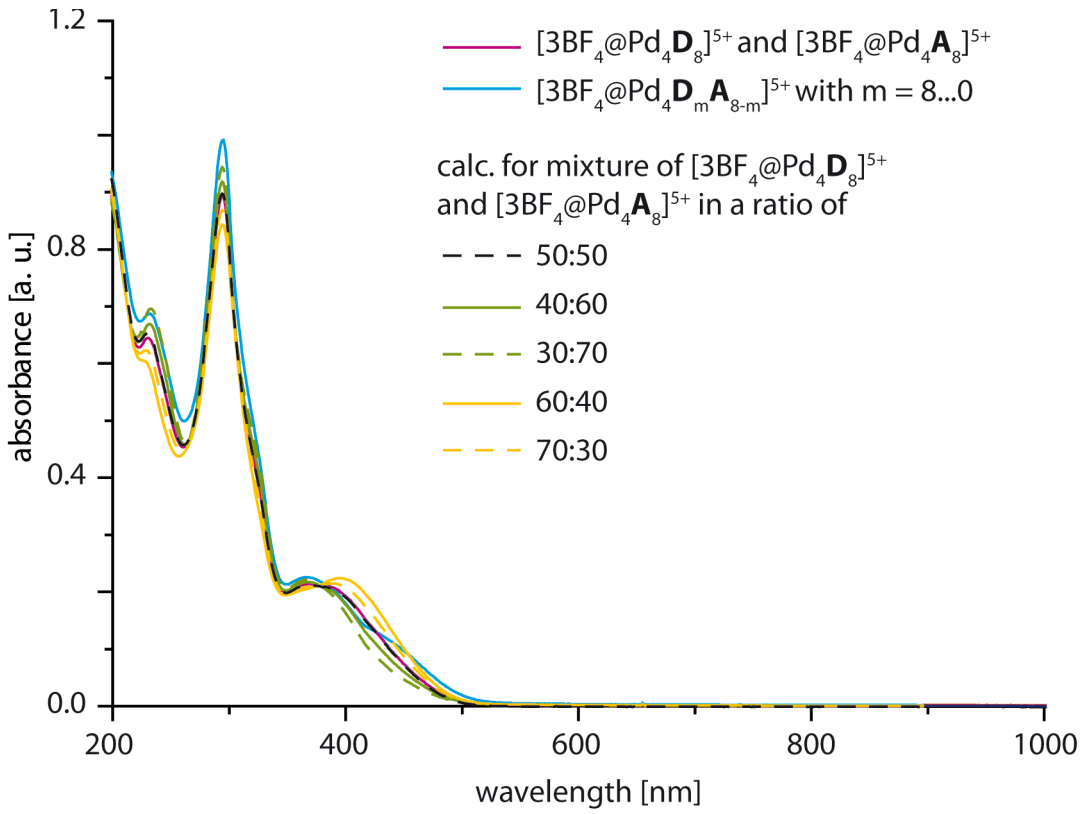

Figure SI-18: UV/Vis spectra of the mixture $[3BF_4@Pd_4\mathbf{D}_8]^{5+}$ + $[3BF_4@Pd_4\mathbf{A}_8]^{5+}$ (10 µM of each double cage in MeCN) and the mixed-ligand cages $[3BF_4@Pd_4\mathbf{D}_m\mathbf{A}_{8-m}]^{5+}$ (20 µM in MeCN). The spectra for the mixture of $[3BF_4@Pd_4\mathbf{D}_8]^{5+}$ and $[3BF_4@Pd_4\mathbf{A}_8]^{5+}$ in ratio of 50:50, 40:60, 30:70, 60:40 and 70:30 have been calculated from experimental spectra of each cage. Cuvette path length: 0.1 cm.

D) Oxidation of the $[3BF_4@Pd_4D_8]^{5+}$ cage

a) UV-Vis spectroscopy

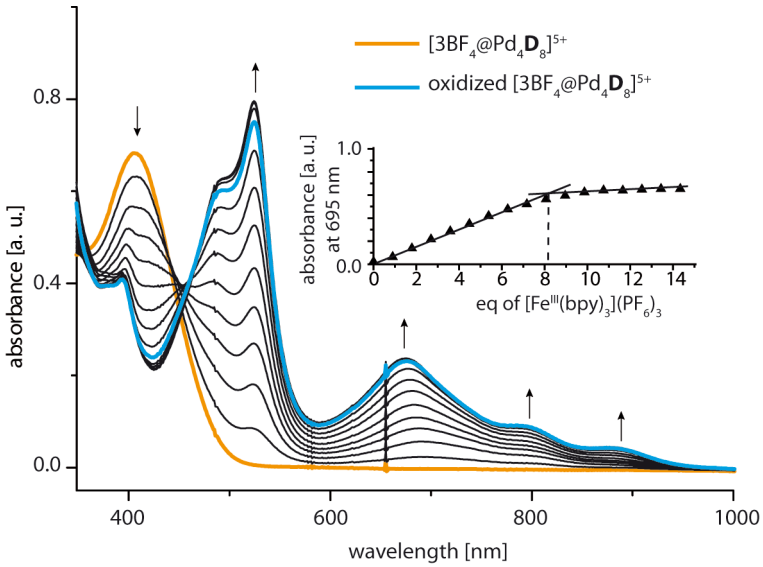

Figure SI-19: Titration of double cage $[3BF_4@Pd_4D_8]^{5+}$ (45 µM in MeCN) with $[Fe(III)(bpy)_3](BF_4)_3$ (2.3 mM in MeCN) followed by UV/Vis spectroscopy. A saturation around the expected value of 8 equivalents can be clearly seen by plotting the absorption at 695 nm over the amount of added oxidant.

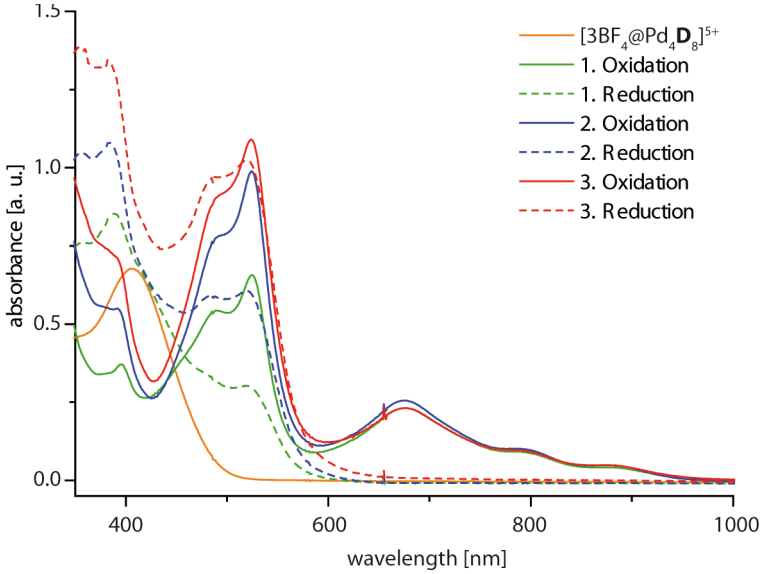

Figure SI-20: Oxidation of double cage $[3BF_4@Pd_4D_8]^{5+}$ (45 µM in MeCN) with $[Fe(III)(bpy)_3](BF_4)_3$ (2.3 mM in MeCN) and subsequent reduction with Zn powder followed by UV/Vis spectroscopy for three oxidation/reduction cycles. In contrast to Figure 4a in the main text, the spectra were not corrected for the additional absorption caused by the $[Fe(II)(bpy)_3]^{2+}$ species that remains in the solution.

b) ^{1}H NMR spectroscopy

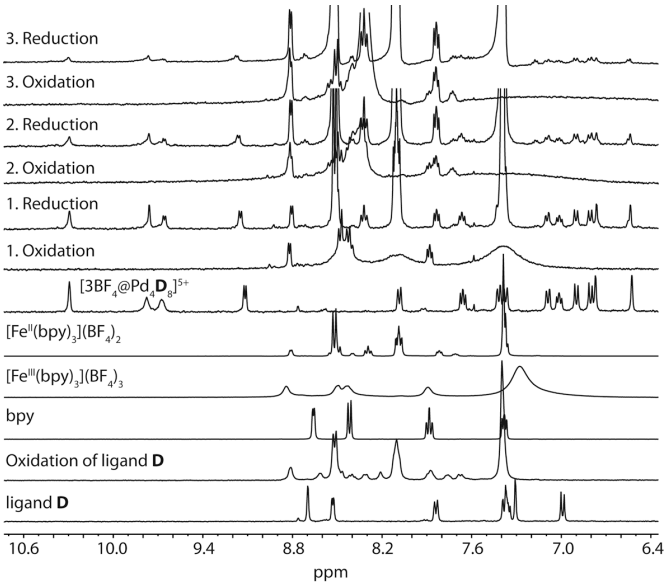

Figure SI-21: ^{1}H NMR (400 MHz, 298 K, acetonitrile-d_3) of free ligand **D**, ligand **D** + $[Fe^{III}(bpy)_3](BF_4)_3$, free 2,2'-bipyridine, $[Fe^{III}(bpy)_3](BF_4)_3$, $[Fe^{II}(bpy)_3](BF_4)_2$, double cage $[3BF_4@Pd_4\mathbf{D}_8]^{5+}$ before starting the oxidation reaction, after first oxidation of $[3BF_4@Pd_4\mathbf{D}_8]^{5+}$ by addition of $[Fe^{III}(bpy)_3](BF_4)_3$, after first reduction by addition of Zn powder and second/third redox cycles.

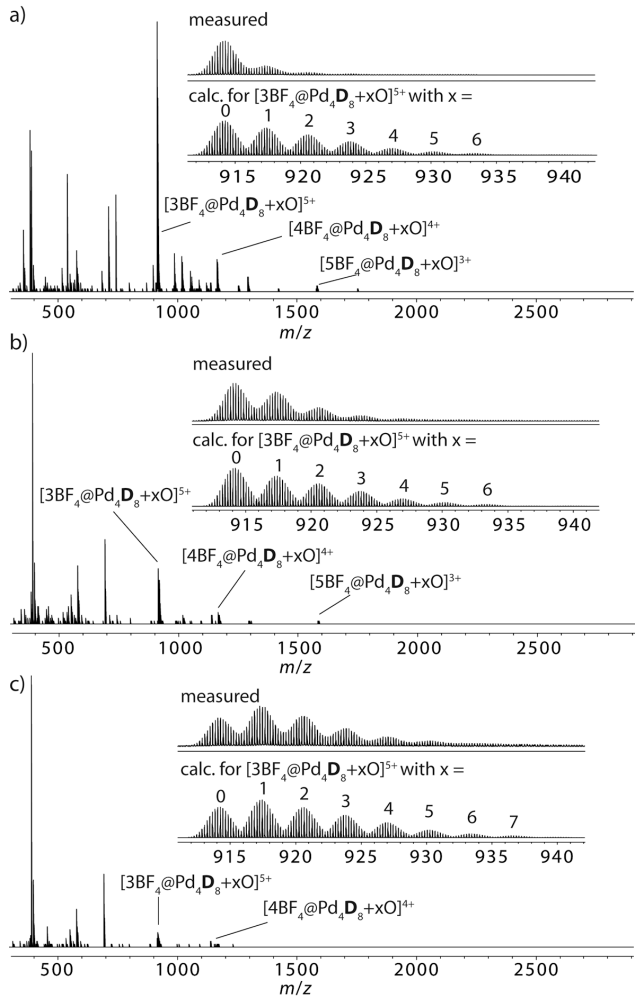

Figure SI-22: ESI high resolution mass spectra of redox cycles of the double cage $[3BF_4@Pd_4\mathbf{D}_8]^{5+}$ measured after each reduction step: a) first, b) second and c) third redox cycle. The creeping oxygenation of the ligands during the redox cycles is caused by traces of water and in accordance with our previous findings (M. Frank, J. Hey, I. Balcioglu, Y.-S. Chen, S. Stalke, T. Suenobu, S. Fukuzumi, H. Frauendorf and G. H. Clever, *Angew. Chem. Int. Ed.* **2013**, *52*, 10102-10106).

E) Cyclic Voltammetry

a) Experimental setup

The cyclic voltammograms were measured with a Metrohm potentiostat PGSTAT101. The data were recorded with the help of the NOVA electrochemistry software (Version 1.9) included in Metrohm Autolab. A homemade electrochemical cell was used for the electrochemical measurements with a minimum sample volume of 3 mL. The sample and electrolyte salt were dissolved in dry and degassed acetonitrile. The electrochemical cell was kept under N_2-atmosphere during the measurements. A glassy carbon electrode was used as working electrode and a Pt wire as counter electrode. After each measurement the glassy carbon electrode and the Pt counter electrode were carefully polished with an appropriate polishing powder and rinsed with acetone and acetonitrile. As reference electrode the non-aqueous electrode $Ag/AgNO_3$ was utilized. For this, a solution of 0.01 M $AgNO_3$ and 0.1 M tetrabutylammonium perchlorate of electrochemical purity grade was prepared in dry and degassed acetonitrile and filled inside the electrode. The reference electrode was kept in acetonitrile/0.1 M tetrabutylammonium perchlorate solution between the measurement and it was rinsed with acetonitrile prior to every measurement. All measurements have been performed at room temperature.

b) CV of ligand D and A and double cages $[3BF_4@Pd_4D_8]^{5+}$ and $[3BF_4@Pd_4A_8]^{5+}$

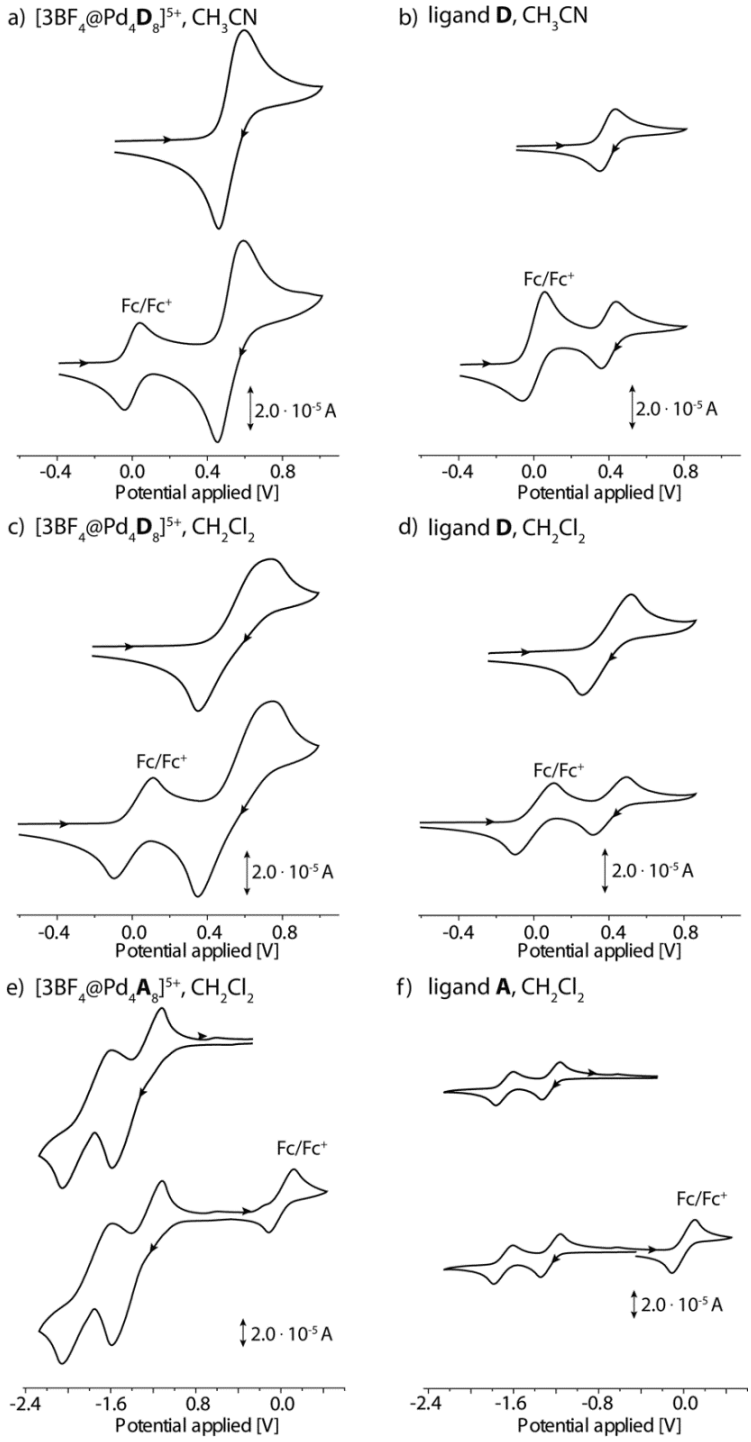

Figure SI-23: Cyclic voltammograms recorded at a glassy carbon working electrode and $Ag/AgNO_3$ reference electrode of a) $[3BF_4@Pd_4\mathbf{D}_8]^{5+}$ (1 mM in CH_3CN), b) ligand **D** (1 mM in CH_3CN), c) $[3BF_4@Pd_4\mathbf{D}_8]^{5+}$ (1 mM in CH_2Cl_2), d) ligand **D** (1 mM in CH_2Cl_2), e) $[3BF_4@Pd_4\mathbf{A}_8]^{5+}$ (1 mM in CH_2Cl_2), f) ligand **A** (1 mM in CH_2Cl_2). The potentials are given with respect to the Fc/Fc^+ potential. Supporting electrolyte: 0.1 M $[NBu_4][PF_6]$. Scan rate: 0.1 $V{\cdot}s^{-1}$. The CV plots of each sample are shown excluding or including ferrocene (1 mM) as internal reference.

c) CV of mixed-ligand cage $[3BF_4@Pd_4D_mA_{8-m}]^{5+}$

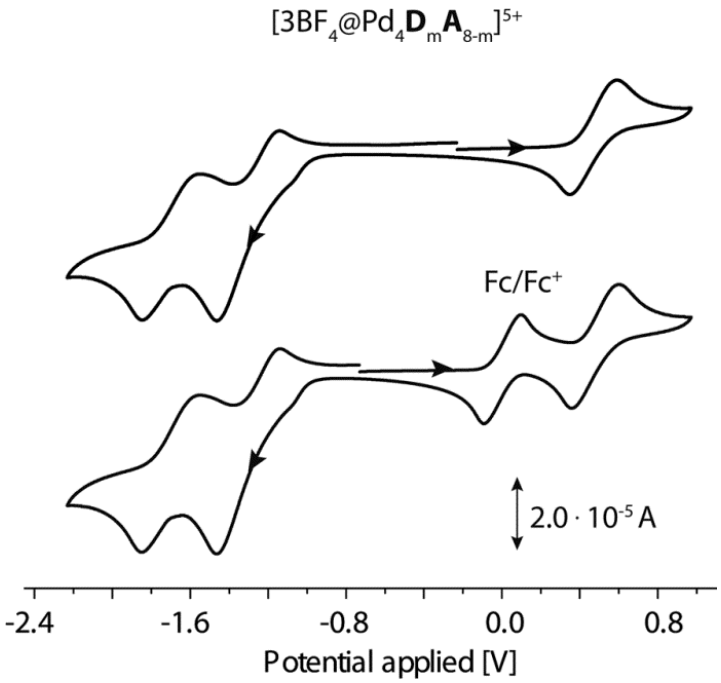

Figure SI-24: Cyclic voltammograms recorded at a glassy carbon working electrode and $Ag/AgNO_3$ reference electrode of the mixed-ligand double cages $[3BF_4@Pd_4\mathbf{D}_m\mathbf{A}_{8-m}]^{5+}$ (1 mM in CH_3CN). The potentials are given with respect to the Fc/Fc^+ potential. Supporting electrolyte: 0.1 M $[NBu_4][PF_6]$. Scan rate: 0.1 $V \cdot s^{-1}$. The CV plots of the sample are shown excluding (top) and including ferrocene (1 mM) as internal reference (bottom).

Table SI1: Cyclic voltammetry parameters.

Compound	scan rate [mV/s]	Solvent	E_f vs $E_{1/2}(Fc/Fc^+)$ [V]	E_r vs $E_{1/2}(Fc/Fc^+)$ [V]	$E_{1/2}$ vs $E_{1/2}(Fc/Fc^+)$ [V]	ΔE [mV]
Ligand **D**	100	CH_3CN	0.43	0.36	0.39	71
	100	CH_2Cl_2	0.49	0.32	0.41	168
$[3BF_4@Pd_4\mathbf{D}_8]^{5+}$	100	CH_3CN	0.59	0.46	0.52	127
	100	CH_2Cl_2	0.70	0.35	0.53	347
Ligand **A**	100	CH_2Cl_2	-1.35 (1) and -1.78 (2)	-1.16 (1) and -1.61 (2)	-1.25 (1) and -1.70 (2)	178 (1) and 171 (2)
$[3BF_4@Pd_4\mathbf{A}_8]^{5+}$	100	CH_2Cl_2	-1.58 (1) and -2.05 (2)	-1.12 (1) and -1.63 (2)	-1.35 (1) and -1.84 (2)	452 (1) and 420 (2)
$[3BF_4@Pd_4\mathbf{D}_m\mathbf{A}_{8-m}]^{5+}$	100	CH_2Cl_2	0.59; -1.45; -1.85	0.37; -1.15; -1.59	0.48; -1.30; -1.72	227; 298; 266

ΔE(Ferrocene): (204±15) mV in CH_2Cl_2 and (85±10) mV in CH_3CN. E_f = forward peak, E_r = reverse peak. (1) first reduction, (2) second reduction step

F) Spectroelectrochemistry

a) Experimental setup

For the spectroelectrochemical measurements a thin layer quartz glass spectroelectrochemical cell was used with an optical path length of 1.0 mm. Instead of a glassy carbon working electrode a Pt mesh electrode was applied. As counter electrode a Pt wire was used. As reference electrode the aforementioned $Ag/AgNO_3$ electrode was used. All spectra were recorded at room temperature. An AvaLight Deuterium-Halogen light source (200 nm - 1000 nm) was used for the UV/VIS measurements. The light was conducted via fiber optic cable (200 µm diameter) to the spectroelectrochemical cell and further to a DAD AVA-SPEC 2048 spectrometer. With every voltage step with a scan rate of 0.01 V/s, the potentiostat PGSTAT101 triggerd the measurement of a full UV-Vis spectrum. The data was recorded and processed using the AVASOFT 7.5 software.

b) Spectroelectrochemical measurements for the ligands D and A, the corresponding homo-octameric double cages $[3BF_4@Pd_4D_8]^{5+}$ and $[3BF_4@Pd_4A_8]^{5+}$ and the mixed-ligand double cages $[3BF_4@Pd_4D_mA_{8-m}]^{5+}$

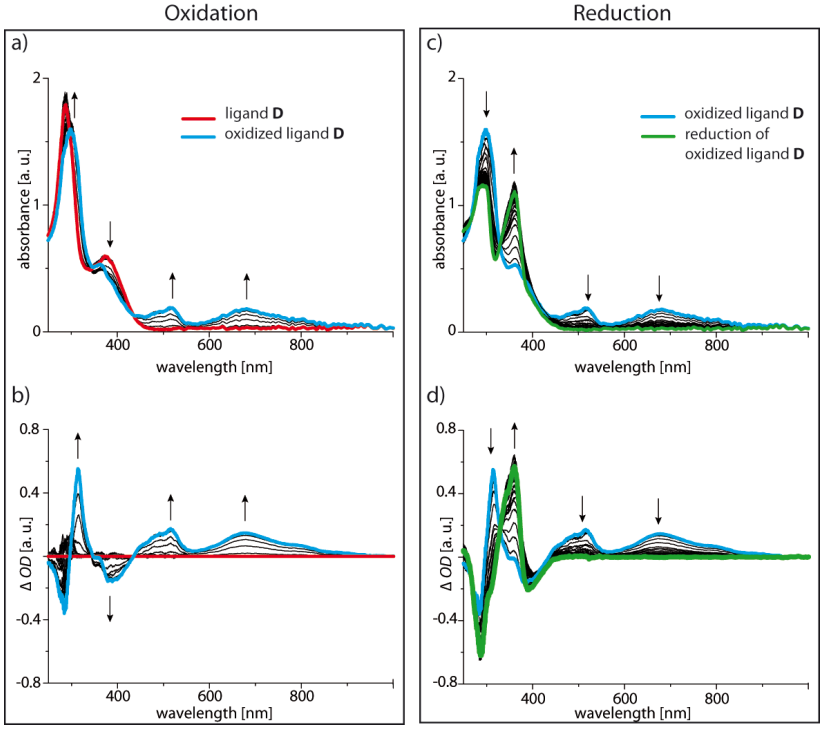

Figure SI-25: UV/Vis spectra of ligand **D** (0.28 mM in CH_3CN, 0.1 M NBu_4BF_4) recorded during cyclic voltammetry with a scan rate of 0.01 $V \cdot s^{-1}$, Pt gauze as working electrode and $Ag/AgNO_3$ as reference electrode. UV/Vis spectra of a) oxidation and c) reduction processes. Optical difference spectra

(compared to initial UV/Vis spectrum of the ligand **D**) are shown for b) the oxidation and d) the reduction process

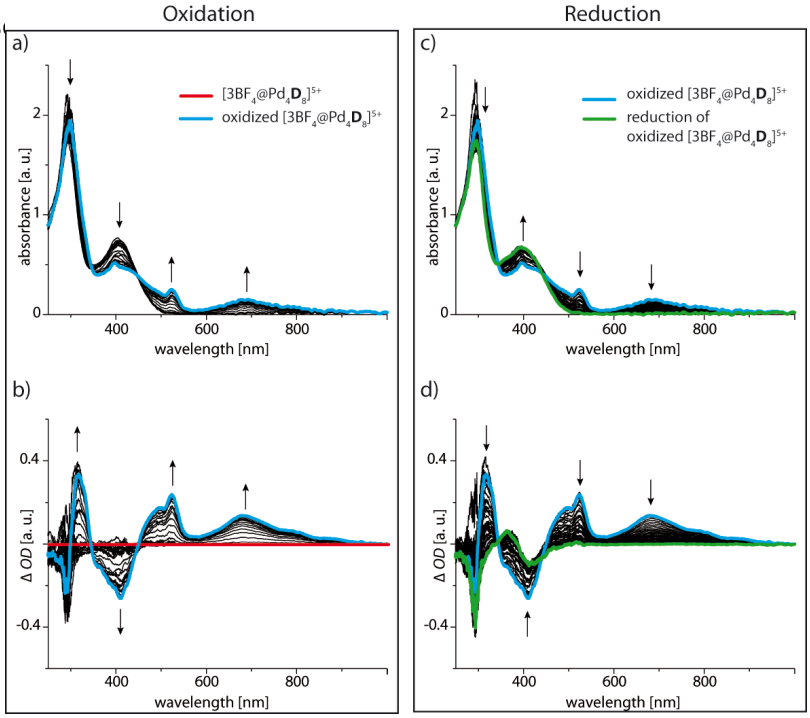

Figure SI-26: UV/Vis spectra of double cage $[3BF_4@Pd_4\mathbf{D}_8]^{5+}$ (0.04 mM in CH_3CN, 0.1 M NBu_4BF_4) recorded during cyclic voltammetry with a scan rate of 0.01 $V \cdot s^{-1}$, Pt gauze as working electrode and $Ag/AgNO_3$ as reference electrode. UV/Vis spectra of a) oxidation and c) reduction processes. Optical difference spectra (compared to initial UV/Vis spectrum of the double cage $[3BF_4@Pd_4\mathbf{D}_8]^{5+}$) are shown for b) oxidation and d) reduction processes.

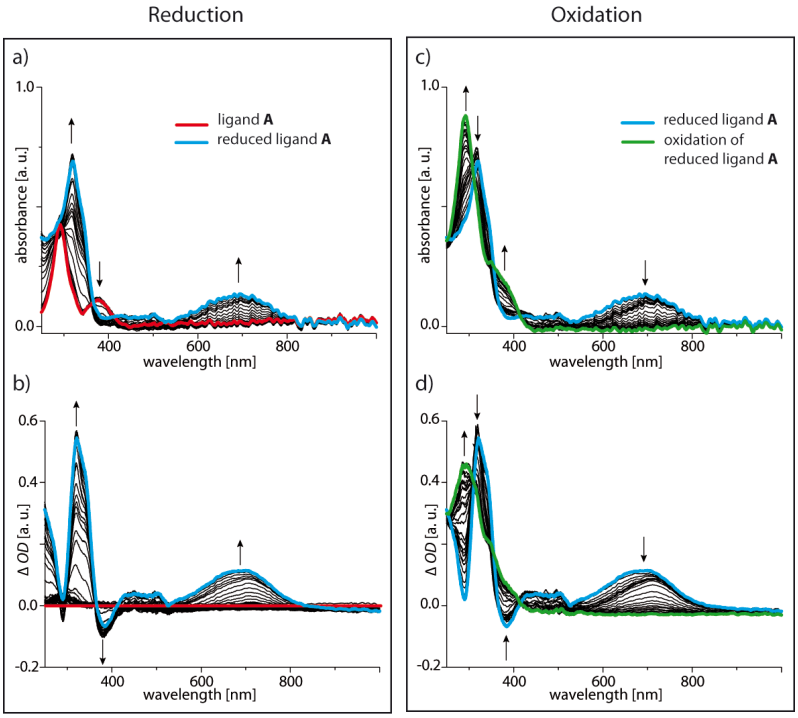

Figure SI-27: UV/Vis spectra of ligand **A** (0.30 mM in CH_3CN, 0.1 M NBu_4BF_4) recorded during cyclic voltammetry with a scan rate of 0.01 $V \cdot s^{-1}$, Pt gauze as working electrode and $Ag/AgNO_3$ as reference electrode. UV/Vis spectra of a) oxidation and c) reduction processes. Optical difference spectra

(compared to initial UV/Vis spectrum of the ligand **A**) are shown for b) oxidation and d) reduction processes.

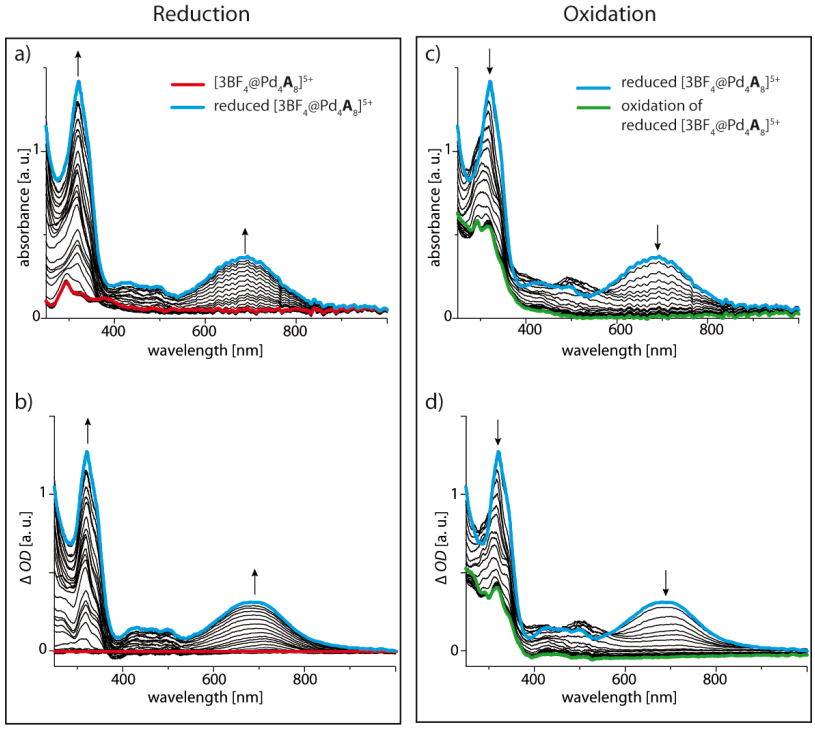

Figure SI-28: UV/Vis spectra of double cage $[3BF_4@Pd_4\mathbf{A}_8]^{5+}$ (0.04 mM in CH_3CN, 0.1 M NBu_4BF_4) recorded during cyclic voltammetry with a scan rate of 0.01 $V \cdot s^{-1}$, Pt gauze as working electrode and $Ag/AgNO_3$ as reference electrode. UV/Vis spectra of a) oxidation and c) reduction processes. Optical difference spectra (compared to initial UV/Vis spectrum of the double cage $[3BF_4@Pd_4\mathbf{A}_8]^{5+}$) are shown for b) oxidation and d) reduction processes.

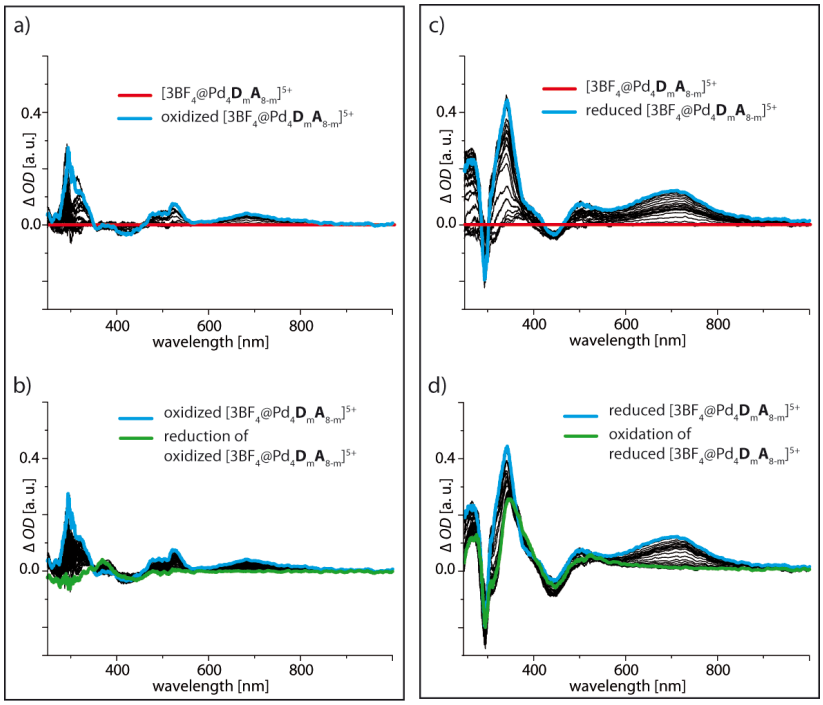

Figure SI-29: UV/Vis spectra of the mixed-ligand double cages $[3BF_4@Pd_4\mathbf{D}_m\mathbf{A}_{8-m}]^{5+}$ (0.04 mM in CH_3CN, 0.1 M NBu_4BF_4) recorded during cyclic voltammetry with a scan rate of 0.01 $V \cdot s^{-1}$, Pt gauze as working electrode and $Ag/AgNO_3$ as reference electrode. Optical difference spectra, compared to

initial UV/Vis spectrum of the ligand, are shown for a) oxidation centered on **D**, b) reduction centered on **D**, c) reduction centered on **A** and d) oxidation centered on **A**.

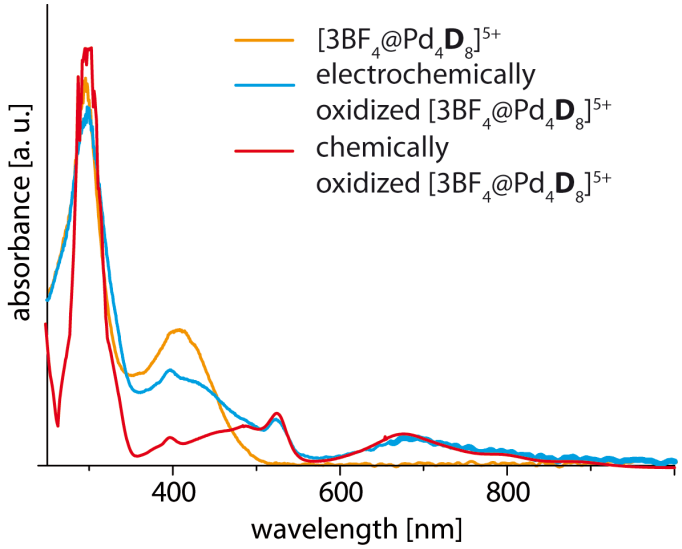

Figure SI-30: Comparison of UV/Vis spectra of electrochemically and chemically oxidized double cage $[3BF_4@Pd_4\mathbf{D}_8]^{5+}$.

G) Transient pump-probe spectroscopy

a) Experimental setup

Transient absorption spectra were measured with a laser system based on a 1 kHz Ti:sapphire regenerative amplifier system (Clark-MXR, CPA-1000) producing 150 fs laser pulses at 775 nm. Pump pulses at 387 nm were generated by second harmonic generation. For excitation in the range 400-440 nm a home-built optical parametric amplifier with subsequent fourth harmonic generation of the idler output was used. Pump pulse energies were attenuated to < 800 nJ and focused to a diameter of about 200 µm at the sample. With a small portion of the 775 nm laser light a white-light continuum was generated in a 4 mm CaF_2 crystal and split into a reference and a probe pulse. The latter was superimposed with the pump pulse at the sample. The relative plane of polarization between pump and probe was set to 54.7° to eliminate over-all molecular rotational effects to the signal. The reference and probe continua were each detected with a 256-element linear diode array attached to a spectrograph. The measured time-dependent transient spectra were corrected with respect to a wavelength dependent shift of the temporal overlap of pump and probe pulses due to group delay dispersion within the white-light-probe continuum. Experiments were performed in a flow cell of 2 mm optical path length equipped with CaF_2 windows. The flow rate was sufficiently high

to exchange the sample in the pump focus between laser shots. For the experiment samples of palladium double cages in acetonitrile were prepared at concentrations of 45 µM.

b) Comparison between mixed-ligand cage and 1:1 mixture of the homo-octameric cages

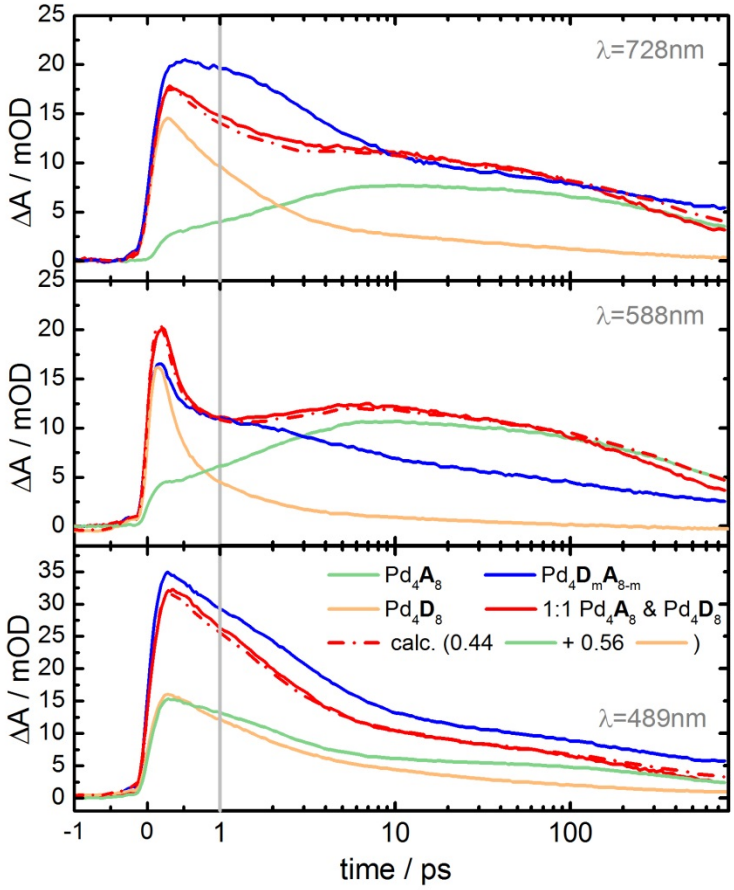

Figure SI-31: Absorption time profiles for the mixed-ligand cage $[3BF_4@Pd_4\mathbf{D}_m\mathbf{A}_{8-m}]^{5+}$ (m = 8…0), the donor and acceptor cages $[3BF_4@Pd_4\mathbf{D}_8]^{5+}$ and $[3BF_4@Pd_4\mathbf{A}_8]^{5+}$, respectively, and a 1:1 mixture of the homo-octameric cages at three selected wavelengths. The signals of the 1:1 mixture (red, full line) can be represented by a weighted sum (red, dash dotted line) of the individual homomeric components (orange and green, respectively) which significantly differ from the mixed-ligand cage signal (blue). (Note: time axis up to 1 ps is linear; above 1 ps it is logarithmic).

References

[1] Patent US2009/0253709A1.
[2] J. Yang, A. Dass, A.-M. M. Rawashdeh, C. Sotiriou-Leventis, M. J. Panzner, D. S. Tyson, J. D. Kinder, N. Leventis, *Chem. Mater*. **2004**, *18*, 3457.
[3] S. Löffler, J. Lübben, L. Krause, D. Stalke, B. Dittrich and G. H. Clever, *J. Am Chem. Soc.* **2015**, *137*, 1060-1063.
[4] Gaussian 09, Revision A.1, M. J. Frisch, G. W. Trucks, H. B. Schlegel, G. E. Scuseria, M. A. Robb, J. R. Cheeseman, G. Scalmani, V. Barone, B. Mennucci, G. A. Petersson, H. Nakatsuji, M. Caricato, X. Li, H. P. Hratchian, A. F. Izmaylov, J. Bloino, G. Zheng, J. L. Sonnenberg, M. Hada, M. Ehara, K. Toyota, R. Fukuda, J. Hasegawa, M. Ishida, T. Nakajima, Y. Honda, O. Kitao, H. Nakai, T. Vreven, J. A. Montgomery, Jr., J. E. Peralta, F. Ogliaro, M. Bearpark, J. J. Heyd, E. Brothers, K. N. Kudin, V. N. Staroverov, R. Kobayashi, J. Normand, K. Raghavachari, A. Rendell, J. C. Burant, S. S. Iyengar, J. Tomasi, M. Cossi, N. Rega, J. M. Millam, M. Klene, J. E. Knox, J. B. Cross, V. Bakken, C. Adamo, J. Jaramillo, R. Gomperts, R. E. Stratmann, O. Yazyev, A. J. Austin, R. Cammi, C. Pomelli, J. W. Ochterski, R. L. Martin, K. Morokuma, V. G. Zakrzewski, G. A. Voth, P. Salvador, J. J. Dannenberg, S. Dapprich, A. D. Daniels, Ö. Farkas, J. B. Foresman, J. V. Ortiz, J. Cioslowski, D. J. Fox, Gaussian, Inc., Wallingford CT, 2009.
[5] K. L. Schuchardt, B. T. Didier, T. Elsethagen, L. Sun, V. Gurumoorthi, J. Chase, J. Li, T. L. J. Windus, *Chem. Inf. Model.* **2007**, 47, 1045-1052.